Supporting Information

Epitope Topography Controls Bioactivity in Supramolecular Nanofibers

Shantanu Sur, Faifan Tantakitti, John B. Matson, Samuel I. Stupp

Department of Material Science and Engineering, Department of Chemistry, Department of Medicine, Department of Biomedical Engineering, Northwestern University, Evanston, IL, 60208 and Simpson Querrey Institute for BioNanotechnology, Northwestern University, Chicago, IL, 60611

Supplementary Movie Legends:

Movie S1. Time lapse observation of fibroblast morphology on G1 PA coated surface. Recording started ~30 min after cell plating and total elapsed time is 5 h 45 min. [Scale bar, 10 μm]

Movie S2. Time lapse observation of fibroblast morphology on G5 PA coated surface. Recording started ~30 min after cell plating and total elapsed time is 5 h 45 min. [Scale bar, 10 μm]

Movie S3. Time lapse observation of fibroblast response to microtubule inhibition on G1 PA coated surface. Total elapsed time is 15 min and the pharmacological inhibitor nocodazole was added after 3 min (corresponds to a dark frame in the movie). [Scale bar, 10 μm]

Movie S4. Time lapse observation of fibroblast response to microtubule inhibition on G5 PA coated surface. Total elapsed time is 15 min and the pharmacological inhibitor nocodazole was added after 3 min (corresponds to a dark frame in the movie). [Scale bar, 10 μm]

Supplementary Figures:

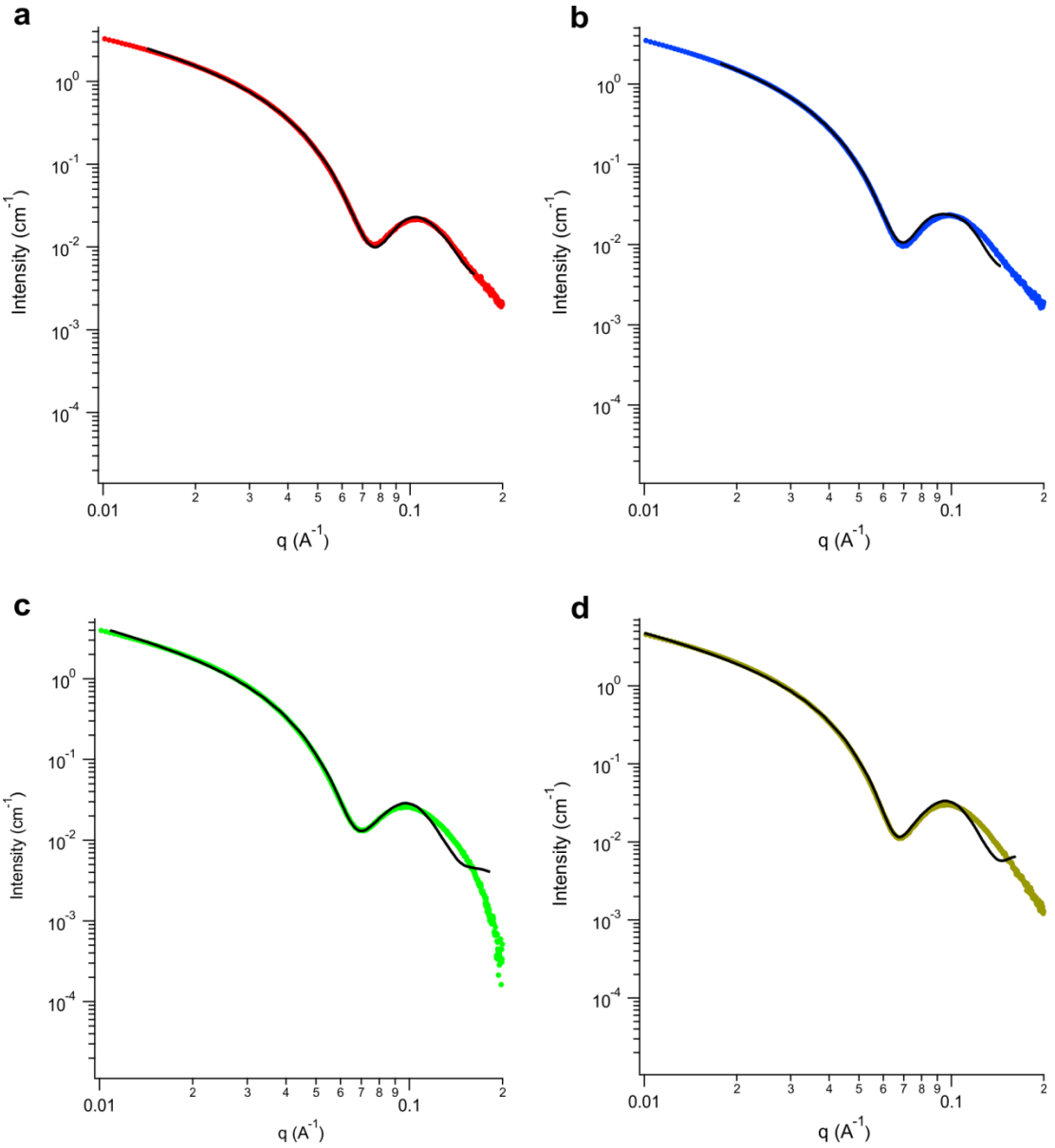

Figure S1. Small angle X-ray scattering (SAXS) spectra of (a) Base PA, (b) G1 PA, (c) G3 PA, and (d) G5 PA are fitted to a poly-disperse core-shell cylinder model (black trace).

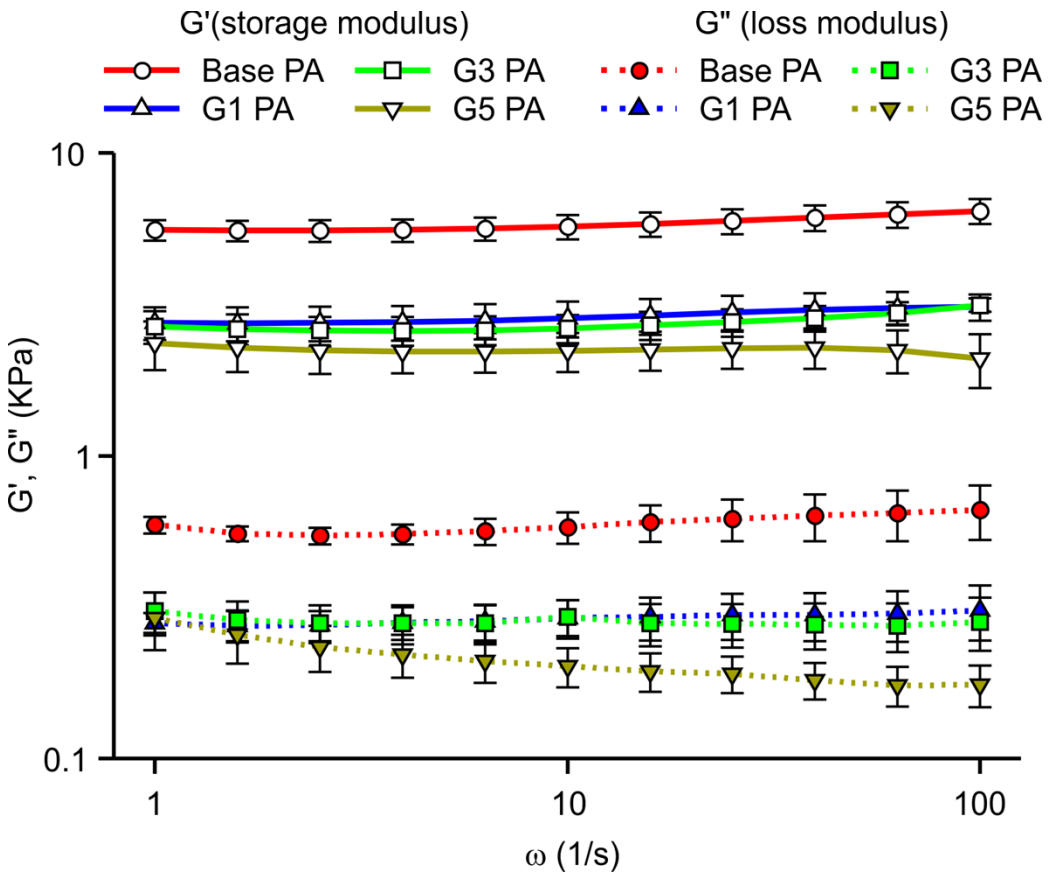

Figure S2. Rheological measurements of PA gels formed at 1% (w/v) over an angular frequency range of 1 to 100 s^{-1} (0.1% strain, n=3)

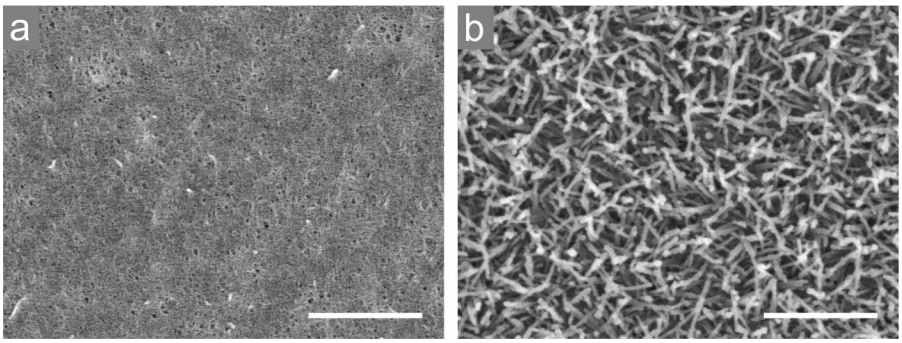

Figure S3. Surface morphology observed by SEM of (a) Ca++ cross-linked alginate layer and (b) subsequent coating of PA nanofibers. The micrographs show a coating of the base PA and represent the coatings of all other PAs used in this study. Scale bar 0.5 μm.

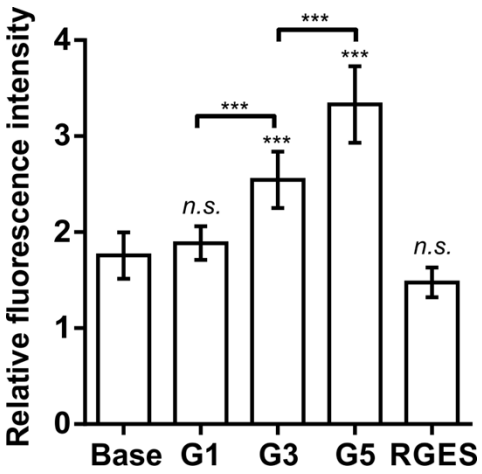

Figure S4. Comparison of cell proliferation on PA nanofiber coated surfaces. 3T3 fibroblasts were cultured on PA-coated substrates for 52 h and cell numbers were quantified by fluorescence intensity measurement using the CyQUANT® assay. To exclude any variability due to initial cell attachment to the substrates, the data was normalized to the fluorescent intensity measured after 4 h of culture. Data represents mean ± SD (*** $p < 0.001$, $^{n.s.}$ $p > 0.05$; calculated against the base PA, unless indicated otherwise, using one-way ANOVA with Bonferroni's multiple comparison post-test; n = 8 for each condition).

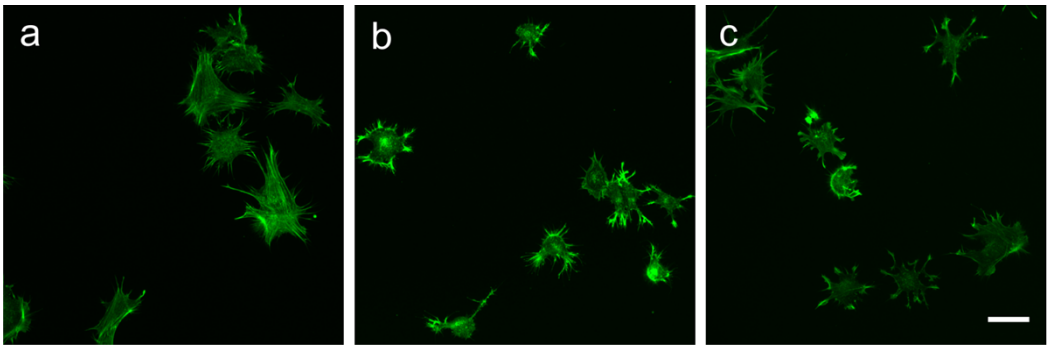

Figure S5. 3T3 fibroblasts were cultured on PA-coated substrates for 5 h and stained for actin (phalloidin staining). Representative morphologies observed on coatings consisted of 10 wt% G5 PA in base PA (a), 10 wt% G5 PA in RGES PA (b), and 100% G5 PA (c). Scale bar 50 μm.

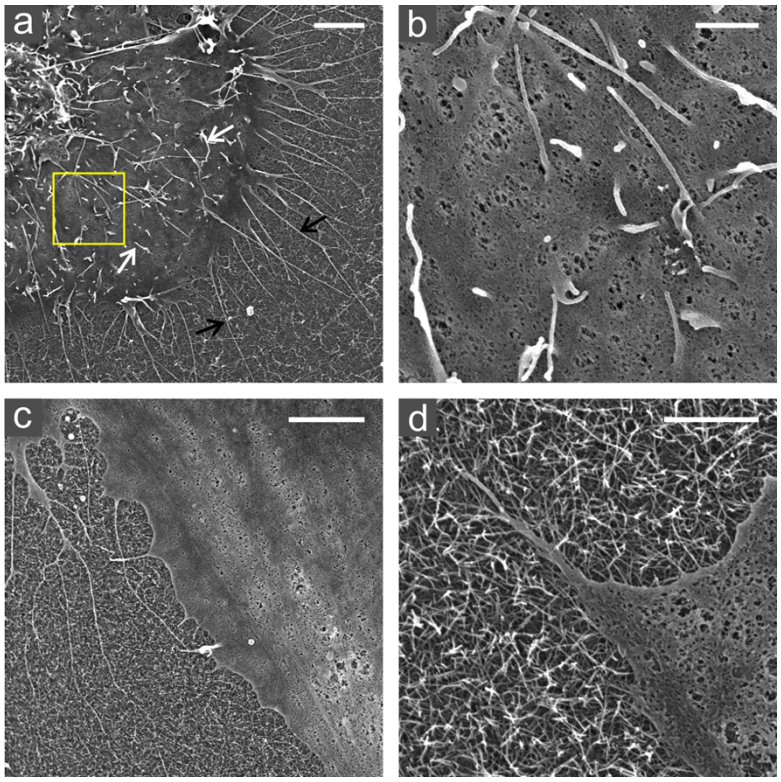

Figure S6. (a-d) Scanning electron micrographs of fibroblasts cultured for 5 h on G1 PA (a,b) and G5 PA (c,d) coated substrates. Black and white arrows in image (a) point to filopodia and filopodia-like processes, respectively. Area enclosed by the yellow square is shown in (b). (c) Filopodial extensions of fibroblasts are also observed on G5 PA coating. (d) Dense network of PA nanofibers on the coating can be observed at higher magnification. Scale bars: a,c 4 μm, b,d 1 μm.

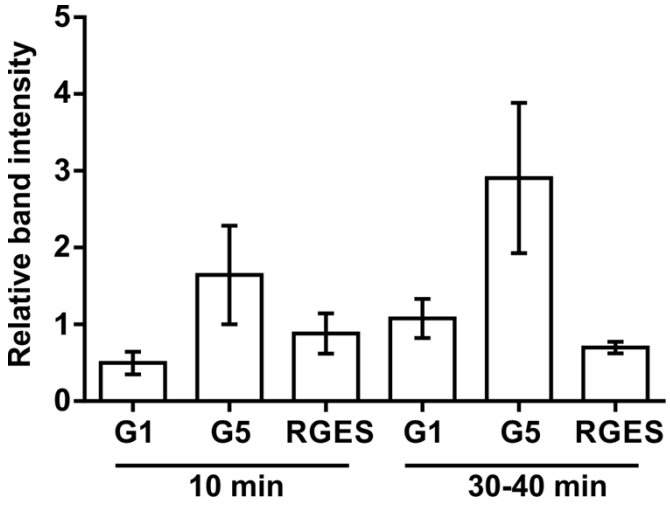

Figure S7. Quantitative densitometry of pFAK expression in fibroblasts measured after incubating for 10 or 30-40 min on PA coated substrates. The band intensity was normalized to GAPDH. Data represents mean ± SEM; n=3.

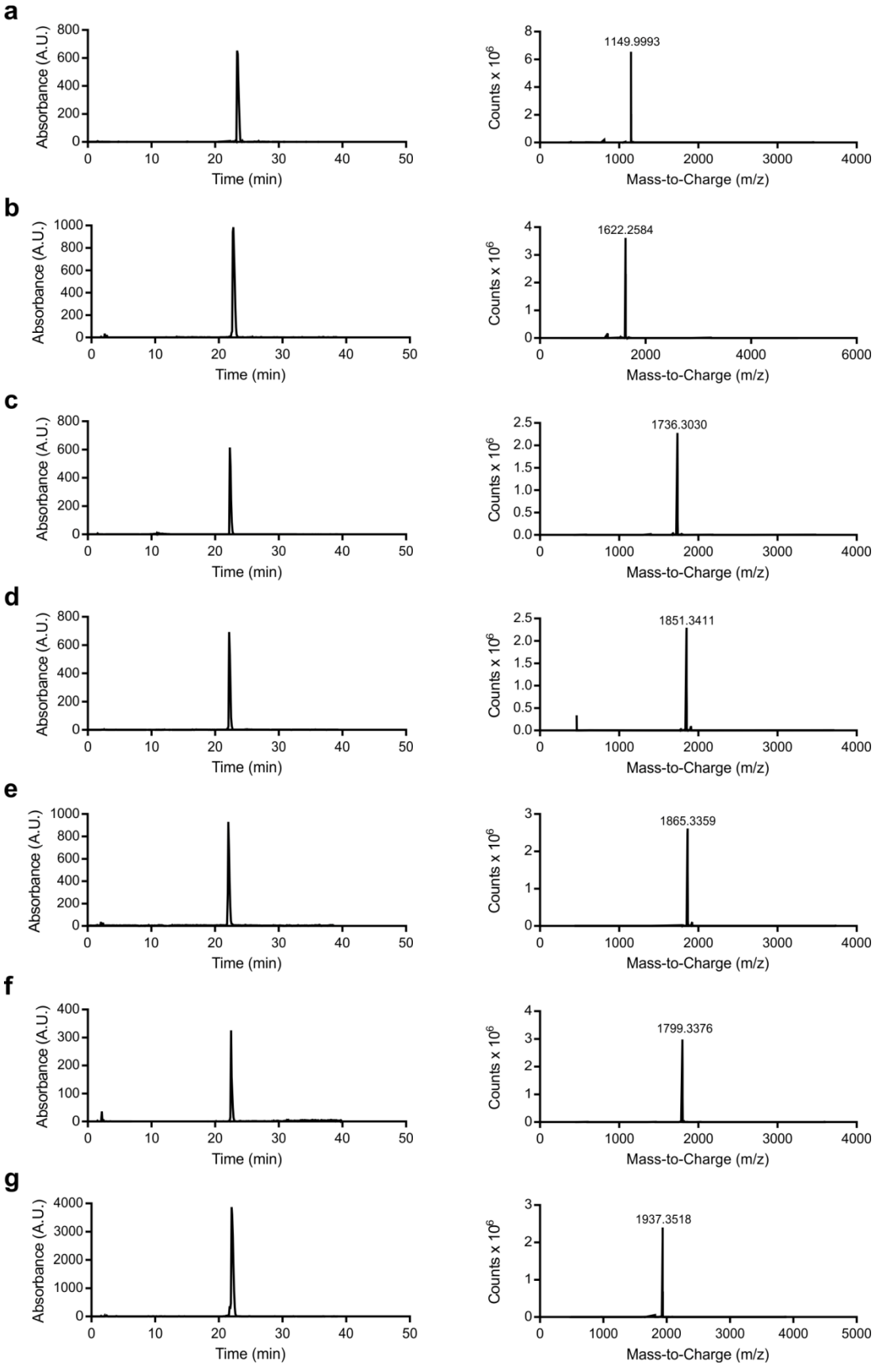
a
Absorbance (A.U.)
Time (min)
1149.9993
Counts x 10^6
Mass-to-Charge (m/z)
b
Absorbance (A.U.)
Time (min)
1622.2584
Counts x 10^6
Mass-to-Charge (m/z)
c
Absorbance (A.U.)
Time (min)
1736.3030
Counts x 10^6
Mass-to-Charge (m/z)
d
Absorbance (A.U.)
Time (min)
1851.3411
Counts x 10^6
Mass-to-Charge (m/z)
e
Absorbance (A.U.)
Time (min)
1865.3359
Counts x 10^6
Mass-to-Charge (m/z)
f
Absorbance (A.U.)
Time (min)
1799.3376
Counts x 10^6
Mass-to-Charge (m/z)
g
Absorbance (A.U.)
Time (min)
1937.3518
Counts x 10^6
Mass-to-Charge (m/z)

Figure S8. Mass determination and characterization of PA molecules. High performance liquid chromatography traces (left) and mass spectrometry (right) of

(**a**) Base PA, MS (*m/z*) $[M]^+$ calc'd. for $C_{58}H_{111}N_{13}O_{10}$, 1149.86; found, 1149.99,

(**b**) G1 PA, MS (*m/z*) $[M]^+$ calc'd. for $C_{75}H_{139}N_{21}O_{18}$, 1622.06; found, 1622.23,

(**c**) G3 PA, MS (*m/z*) $[M]^+$ calc'd. for $C_{79}H_{145}N_{23}O_{20}$, 1736.10; found, 1736.30,

(**d**) G5 PA, MS (*m/z*) $[M]^+$ calc'd. for $C_{83}H_{151}N_{25}O_{22}$, 1850.15; found, 1851.34,

(**e**) RGES PA, MS (*m/z*) $[M]^+$ calc'd. for $C_{84}H_{153}N_{25}O_{22}$, 1864.16; found, 1865.34,

(**f**) Flexible PA , MS (*m/z*) $[M]^+$ calc'd. for $C_{83}H_{155}N_{21}O_{22}$, 1798.17; found, 1799.34,

(**g**) Rigid PA, MS (*m/z*) $[M]^+$ calc'd. for $C_{95}H_{153}N_{23}O_{20}$, 1937.17; found, 1937.35.